

Metals Accumulation and Leaf Surface Anatomy of *Murdannia spectabilis* Growing in Zn/Cd Contaminated Soil

Ladawan Rattanapolsan, Woranan Nakbanpote and Piyaporn Saensouk

Department of Biology, Faculty of Science, Mahasarakham University, Khamriang, Kantarawichi District, Maha Sarakham 44150, Thailand.

Abstract

Murdannia spectabilis (Kurz) Faden was identified as a Zn/Cd hyperaccumulative plant. Leaf surface anatomy of the plant growing in non-contaminated soil (control) and Zn/Cd contaminated soil, was studied and compared by a light microscopy and scanning electron microscopy combined with Energy-dispersive X-ray spectroscopy (SEM/EDS). The similarities were reticulate cuticle on epidermises, uniform polygonal cell, stomatal arrangement in six surrounding subsidiary cells, and submarginal sclerenchyma. The dissimilarities were uniseriate trichomes spreading on both adaxial and abaxial epidermis of the plants growing in non-contaminated soil, whereas the uniseriate trichomes were only on the submarginal-adaxial epidermis of the control plants. The trichomes on leaves of the plants growing in non-contaminated soil were found to have both uniseriate non-glandular and uniseriate glandular trichomes; whereas, leaves of the plants growing in the contaminated soil were merely non-glandular trichomes. The different shape and location of trichomes, the number of stomata and trichome indicated the effect of Zn and Cd on *M. spectabilis*. The higher percentages of Zn and Cd in the vascular bundle than in the cross section and epidermis areas showed both solutes could move along each route, with diffusion through the symplast and apoplast. The increase of Ca in *M. spectabilis* growing in Zn/Cd contaminated soil corresponded to the Zn and Cd distributed in the leaves. Zn K-edge and S K-edge XANES spectra proposed that Zn²⁺ ions were accumulated and/or adsorbed on the epidermis of the tuber, and then absorbed into the root and transport to the xylem. The double peaks of Zn-cysteine in the leaf samples proposed the metal sequestration was by sulphur proteins.

Keywords: anatomy; cadmium; phytoremediation; *murdannia*; zinc

1. Introduction

Metal pollution problems occur when human activity either disrupts the normal biogeochemical cycles or concentrates metals; examples of such activities include mining and ore refinement (Kabata-Pendias and Pendias, 1992; Roane *et al.*, 1996). Metal wastes can exist as individual metals or, more often, as metal mixtures. Cadmium (Cd) never occurs in isolation in natural environments but, rather, appears mostly as a “guest” metal in zinc (Zn) mineralisation (Baker *et al.*, 1990). The typical background levels of Cd and Zn in non-contaminated soil were 0.02-2 mg/kg and 1-900 mg/kg, respectively (Alloway, 1995; Bowen, 1979). Soil in the fields of Phatat Phadaeng sub-district, Mae Sot, Tak Province, Thailand, is a source of Zn mineralisation. The total soil Cd concentrations in Mae Sot were positively correlated with total soil Zn concentrations (Simmons *et al.*, 2005; 2009). The total Cd and Zn concentrations in the rice fields, forest and mining areas were approximately 64-1,458 mg Cd/kg and 2,733-57,012 mg Zn/kg, respectively (Phaenark *et al.*, 2009). Both Zn and Cd accumulated to toxic concentrations in soil resulting in significant risk to the health of

natural ecosystem (Prasad, 1995; Chaney, 1993). Our exploration of a Zn mine area uncovered *Murdannia spectabilis* that accumulated high levels of Zn and Cd. The plants were frequently found nearby *Gynura pseudochina* (L.) DC., a Zn/Cd hyperaccumulative plant (Panitlertumpai *et al.*, 2003; 2013).

To be an efficient metal accumulator, plants require efficient detoxification and tolerance mechanisms at both the cellular and plant level. The general processes of metal accumulation in plants include the uptake of metals from the soil, sequestration within the root, efficient xylem loading and transport, and storage in the leaf cells (Rascio and Navari-Izzo, 2011). The stress of metal toxicity in plants often causes the expression of metal-induced alterations in leaf morphology. Microscopic structural changes, such as a decrease in intercellular spaces and shrinkage of palisade and epidermal cells, occurred in leaves of barley (*Hordeum vulgare*) plants treated with high concentrations of Zn (Sridhar *et al.*, 2007). The leaf surface of *Helianthus annuus* L., grown on tannery sludge containing high Cr, Fe, Zn and Mn levels, showed an increase in the frequency of stomata and trichomes, closure of stomata and degeneration of certain cells (Singh and

Sinha, 2004). The accumulation of Cd and Zn in *Picris divaricate* was in larger trichomes and epidermal cells (Hu et al., 2012; Broadhurst et al., 2013). In tobacco (*Nicotiana tabacum* L.), Cd and Zn caused an increase in the number of trichomes (Choi et al., 2001; Sarret et al., 2006). The roles for Cd-detoxification in tobacco were Cd-Ca crystal formation as a metal substituted calcite and sulfur accumulated on the head cells of short glandular trichomes (Choi et al., 2001; 2004; Harada and Choi, 2008). Sequestration of Cd in trichomes was found in *Arabidopsis thaliana* and *Arabidopsis halleri*, Cd existed in the divalent state and was bound to the O and/or N ligands (Isaure et al., 2006; Fukuda et al., 2008), and a minor fraction could be bound to S-containing ligands (Isaure et al., 2006). The Zn sequestration in *A. halleri* was at the base of the trichomes (Zhao et al., 2000), in which Zn was tetrahedrally coordinated and complexed to carboxyl and/or hydroxyl functional groups (Sarret et al., 2002). However, trichomes were not the only sink for Zn and Cd in *A. halleri*, mesophyll cells also accumulated substantial amounts of both metals (Küpper et al., 2000).

There have been no detailed studies on Zn/Cd accumulation in *M. spectabilis*. Therefore, this research aims to study the accumulation of Zn and Cd, and investigate some morphological changes caused by Zn and Cd accumulation in leaves of *M. spectabilis*. To correlate metal accumulation with anatomical and morphological changes, the leaf anatomy was investigated by a light microscopy and scanning electron microscopy (SEM) combination with Energy-dispersive X-ray spectroscopy (EDS). X-ray absorption near-edge structure (XANES) was carried out to determine the oxidation state and probable coordination of Zn and S in the plant samples.

2. Materials and Methods

2.1. Plant materials

M. spectabilis (Kurz) Faden (Fig. 1) is in the Comelinaceae family and is found throughout Thailand. It

is a monocotyledon, perennial herbs, with basal rosettes, leaf blade linear; cauline leaves with blade similar in shape and size to that of basal leaves, or smaller. Stem erect tall (including inflorescences). The roots are thin to moderate thickness, ellipsoid or subdistal tubers, rhizomes absent. The flower is purple to violet-blue, slightly zygomorphic (Thitimetharoch, 2004; Shu, 2000). The plants and Zn/Cd contaminated soil samples were collected from a zinc mining area, Phatathadaeng sub-district, Mae Sot, Tak Province, Thailand in August 2011 (Site: N 16° 39' 6.6"E 98° 39' 41.2").

2.2. Pot experiments

M. spectabilis was grown and propagated in a greenhouse, Maha Sarakham, Thailand. Young plant with 2-3 swollen roots (tubers) were separated into two groups for growth in the Zn/Cd soil sample and non-contaminated soil (control). The non-contaminated soil was prepared by mixing, in a ratio of 1:2, fertile soil to non-contaminated soil, which was obtained from Ban Chiang Hian, Maha Sarakham, Thailand. The characteristics of the soil samples are shown in Table 1. The plants were grown in the greenhouse for five months (July-November 2012) before harvesting. The temperature and humidity during the experiments were 20-36°C and 36-78%, respectively.

2.3. Leaf anatomical studies

The lower second of the basal leaves were used for anatomical studies. Fresh mature healthy leaves were fixed in formalin: acetic acid: 70% alcohol (5:5:90) for 18-24 hours. The central portions of the mature laminae were taken as samples for leaf-scrapes and free hand transverse sectioning. The samples were stained with safranin and made into permanent slides according to Johansen (1940). The slides were observed by light microscopy (CH30 Olympus, Japan). Photographs were obtained using a digital eyepiece camera (DEM200-Scope Tek, China), then analysed using ScopePhoto Version 3.1.475 software. The density of stomata in the



Figure 1. *Murdannia spectabilis* (a) flowers, (b) leaves and (c) roots and swollen roots.

Table 1. Soil texture, quantities of elements and concentration of zinc and cadmium

Characteristics of soil		Soil sample	
		Zn/Cd contaminated soil	Non-contaminated soil
Soil texture (%)	Sand	74.34±2.88	74.09±1.65
	Silt	9.25±1.34	8.98±1.32
	Clay	16.41±3.45	16.93±2.71
Quantities of elements (%)	Nitrogen (N)	0.60±0.36	0.84±0.28
	Carbon (C)	2.94±0.43	4.55±1.47
	Hydrogen (H)	0.27±0.05	0.16±0.02
	Sulfur (S)	1.61±0.02	1.64±0.03
	Oxygen (O)	8.03±0.07	5.54±0.73
Metal concentration (mg/kg dry weight)	Total Zn	42,570.73±2,300.36	36.96±7.49
	Extractable Zn	1,289.81±223.67	13.21±0.34
	Total Cd	68.44±2.61	1.86±0.54
	Extractable Cd	8.65±0.85	0.02±0.02

Mean values ($n = 3$) ± standard deviation (S.D.).

margins and midrib of the leaf samples were counted in a rectangular area of 0.88 mm² (0.8 mm x 1.1 mm). The opening stomata cells and non-glandular trichomes in the margins and midrib of the leaf samples were measured for length.

The healthy plants were harvested and washed with an excess of running deionised water. The cross sections of the tuber and leaves were cut to a thickness of 200-300 µm using a clean stainless-steel razor and immediately placed on dry ice. The sections were freeze-dried overnight using a lyophiliser (Heto Power Dry PL3000, Japan). The sections for SEM images were put on carbon tape on aluminium stubs, then coated with a thin layer of carbon by a coater (SPI-Module TM sputter coater, Japan) and examined with a SEM (JEOL-JSM 6460LV, Japan). The Zn and Cd distribution in the plant samples were determined on uncoated sections by SEM coupled with EDS (Inca x-sight Oxford Instrument, UK).

2.4. XANES analyzes

The harvested plants were washed with an excess of running deionised water, and then the plants were separated into the swollen root (tuber) and leaves. The separated samples were freeze-dried using the lyophiliser. The dried tuber was separated to epidermis (TU-E) and cortex plus vascular cylinder (TU-I). For bulk XANES analysis, an amount of each freeze-dried plant part (tuber (TU-E and TU-I) and leaves) was ground to a homogenized powder by a ball mill grinder (Mini-Mill pulverisette 23 Fritsch, Germany). A sample of the powder was thinly smeared on sticky Kapton tape (LanmarInc., USA). XANES spectra of the Zn

K-edge and S K-edge were performed at beamline 8, Synchrotron Light Research Institute (Public Organization), Thailand. XANES spectra were collected by fluorescence X-ray detector of 13-Channel Germanium detector (GeD), at room temperature. Double crystal monochromators for Zn and S were Ge (222) and InSb (111), respectively. The focusing mirror was a bending magnet, and beam size was 10 mm(h) x 1 mm (v). To obtain a good signal-to-noise ratio, the I₀ ion chamber (10-cm-long) and I₁ ion chamber (40-cm-long) were filled with specified gas mixtures and pressure for Zn (I₀: Ar 93 mbar, I₁: Ar 509 mbar) and S (I₀: N₂37 mbar, I₁: N₂200 mbar). The atmosphere in the sample chamber was air. XANES spectra were analyzed using Athena under IEFIT version 1.2.9. The reference chemicals were ZnSO₄, ZnO, ZnS and ZnCl₂, and adsorption techniques were used to prepare the Zn-cysteine, Zn-glutathione and Zn-methionine reference materials (Panitlertumpai *et al.*, 2013).

2.5. Soil analyzes

The soil sample was analyzed for the total carbon, hydrogen, nitrogen, sulphur and oxygen content by a CHNS/O analyzer (LecoTruSpec Micro, USA). To determine the total concentrations of Zn and Cd in the soil samples, 0.1 g of each sample was digested in aqua regia (the mixture of 35% (w/v) HCl and 70% HNO₃ as 3:1). The digestion method was adapted from ASTM E841-04 (ASTM, 2004). The extractable concentrations of Zn and Cd in soil were determined by shaking the soil at 150 rpm for 2 hours in 0.005 M diethylene triamine penta acetate (DTPA) using a soil : extractant ratio of 1:2 following the modified method of Lindsay

and Norvell (1978). The total and extractable metal concentrations were measured by an Atomic Absorption Spectrophotometer (AAS) (Shimadzu AA-680, Japan).

2.6. Plant analyzes

A plant sample was collected and divided into the root and shoot parts, the sample was rinsed with tap water, washed three times with deionized water and oven-dried at 80°C. Each dried sample was digested with HNO₃ conc (70% v/v) and HClO₄ (70% v/v) by a modified method of Miller (1998). The digested sample was analyzed for Zn and Cd concentrations by AAS. Translocation factor (*TF*) was calculated from the metal concentration in the plant shoots (leaves and stem) divided by the metal concentration in the plant roots, and bioaccumulation factor (*BF*) was calculated from the metal concentration in the shoots divided by the extractable concentration of metal in the soil around the plant roots (Phaenark et al., 2009).

2.7. Data analysis

Data was expressed as means with standard deviation (SD). The data obtained was analysed using a one-way analysis of variance (one-way ANOVA) at $p < 0.01$. The statistical analysis was performed using the SPSS Version 11.5 software program (SPSS Inc., USA).

3. Results and Discussion

3.1. Zn and Cd concentration in soil and plant

The Zn/Cd soil sample collected from Mae sot, Tak Province, Thailand (Table 1) was sandy loam soil. The CHNO/S analysis showed the soil contain a little nitrogen and sulfur, the amounts were enough for plant growth (Baber, 1995). The soil contained high total Zn and Cd at 42,570 and 1,290 mg/kg dry weight, respectively. The available Zn and Cd concentrations were 1,290 and 8.65 mg/kg dry weight, respectively, which

were obviously higher than the Zn and Cd levels with respect to optimal plant growth (70-400 mg Zn/kg and 3-8 mg Cd/kg) (Kabata-Pendias and Pendias, 1992). Non-contaminated soil was prepared that had nearly the same properties as the Zn/Cd soil, except for the metals contamination. The total and extractable Zn and Cd in the non-contaminated soil were lower than background levels of Zn and Cd in a non-contaminated soil reference (1-900 mg Zn/kg and 0.02-2 mg Cd/kg) (Alloway, 1995; Bowen, 1979).

M. spectabilis growing in the contaminated soil was able to translocate and accumulate Zn and Cd in the shoots and above ground parts of the plant. Zn and Cd accumulated in the shoot (stem and leaves) were 2,067.1 mg/kg dry weight and 26.7 mg/kg dry weight, respectively (Table 2). The translocation factor (*TF*) of Zn and Cd were 1.8 and 1.4, respectively, and the bioaccumulation factor (*BF*) of the Zn and Cd were 1.6 and 3.1, respectively. The criteria for Zn and Cd hyperaccumulative plants are (1) the concentration of Zn and Cd in above-ground biomass is 10-500 times more than that in a usual plant (Zn 100 mg/kg dry weight; Cd 1 mg/kg dry weight) (Baker and Whiting, 2002); (2) Zn and Cd concentrations in shoots are invariably greater than that in the roots ($TF > 1$); and (3) the ratio of Zn and Cd concentration in plant shoots to the extractable concentration of Zn and Cd in the soil ($BF > 1$) (Braquinho et al., 2007; González and González-Chávez, 2006). From the criteria for a Zn/Cd hyperaccumulator, *M. spectabilis* could be classified as a Zn/Cd hyperaccumulative plant. In addition, plants growing in the non-contaminated soil were suitable for use as control samples for anatomical study because of slight Zn and Cd accumulation.

3.2. Leaf anatomy

Leaf-blade anatomy in *M. spectabilis* growing in non-contaminated soil (control) is showed in Fig. 2. The epidermis is composed of uniform, polygonal with elongated cells over the veins on both the adaxial and abaxial epidermises [Fig. 2(a)]. There was reticulate cuticle on both epidermises. Hexacytic stomata [Fig. 2(c)], which

Table 2. Zinc and cadmium accumulation, translocation factor (*TF*) and bioaccumulation factor (*BF*) of *M. spectabilis*, growing in Zn/Cd contaminated and non-contaminated soils.

Soil treatments	Zn accumulation (mg/kg dry weight)		Cd accumulation (mg/kg dry weight)		<i>TF</i>		<i>BF</i>	
	Shoot	Root	Shoot	Root	Zn	Cd	Zn	Cd
Zn/Cd contamination	2,067±74	1,148±71	26.7±1.2	20.2±4.2	1.8±0.1	1.4±0.3	1.6±0.3	3.1±0.4
Non-contamination	11.4±3.5	18.3±5.4	2.8±1.6	5.2±2.7	-	-	-	-

Mean values ($n = 3$) ± standard deviation (S.D.).

is a stomatal arrangement of six surrounding subsidiary cells, were scattered on the abaxial epidermis and the submarginal adaxial epidermis. Fig. 2(g) shows uniseriate non-glandular and glandular trichomes spreading on both adaxial and abaxial epidermises, and submarginal sclerenchyma. In comparison with *M. spectabilis* growing in Zn/Cd contaminated soil, the similarities are reticulate cuticle on the adaxial and abaxial epidermises, uniform polygonal cells [Fig. 2(b)], hexacytic stomata [Fig. 2(d)] and submarginal sclerenchyma [Fig. 2(h)]. The dissimilarities were the trichomes spreading on both adaxial and abaxial epidermises of the plants' leaves growing in non-contaminated soil, whereas trichomes of the plants growing in Zn/Cd contaminated soil were only on the submarginal-adaxial epidermis [Figs. 2(g), 2(h)]. In addition, non-glandular and glandular trichomes were found on the leaves of the plants growing in non-contaminated soil [Fig. 2(e)], whereas the trichomes on the leaves of plants growing in the contaminated soil were merely non-glandular trichomes [Fig. 2(f)]. The decrease in stomata density and increase in stomata size on the plants' leaves growing in Zn/Cd contaminated soil was indicated by a comparison with the control plants. While there were no differences in the size of the trichomes between both groups (Table 3).

The SEM images of trichomes on the plants' leaves growing in non-contaminated and Zn/Cd contaminated soils are shown in Fig. 3 and Fig. 4, respectively. They indicated the effect of Zn and/or Cd on the different trichome shapes of *M. spectabilis*. A transverse section of the midrib region [Fig. 3(a)] shows non-glandular trichomes and glandular trichomes on both the adaxial and abaxial epidermises, similar to the margin of the adaxial and abaxial epidermises, respectively [Figs. 3(b), 3(c)]. The high magnification in Figs. 3(d) and 3(f) clearly shows non-glandular trichomes and glandular trichomes, respectively. In contrast, Fig. 4(a) shows the trichome was absent from the midrib region of *M. spectabilis* leaves growing in the contaminated soil. The non-glandular trichomes were found on the margin-adaxial epidermis [Figs. 4(b), 4(d)]. Although Fig. 4(c) shows the absence of trichome on the margins-abaxial epidermis, the high magnifying image shows the evidence of abnormal flattening of trichomes [Fig. 4(e)].

The distribution of Zn and Cd in the leaves of *M. spectabilis* growing in Zn/Cd contaminated and non-contaminated soil was investigated using SEM/EDS (Table 4). The percentages of Cd in the areas of the epidermis and vascular bundle were 0.1% and 0.3%, respectively. The percentage of Zn in the areas of the epidermis and vascular bundle were 0.02% and 0.2%, respectively. While Cd and Zn signal were not detected in the leaves of *M. spectabilis* growing in non-contaminated soil (control). The percentages of Mg, Si, and Cl in the cross section area of the plant's leaves growing in Zn/Cd contaminated soil were lower than the percentages of the elements found in the control plant sections, whereas the percentage of Ca was noticeably higher.

The microscopic studies showed the effect of Zn and Cd on the morphology of the leaves of *M. spectabilis*. The evidence showed decreased stomata density, increased stomata size and especially the spreading and shape of trichomes on the adaxial and abaxial epidermises. In contrast with sunflower, the plants growing in tannery sludge (containing Cr, Fe, Zn and Mn) showed an increase in the frequency of stomata and trichomes (Singh and Sinha, 2004). Trichomes are specialized unicellular or multicellular structures derived from the epidermal cell layer, which may have various functions depending on the plant species and organ (Rodriguez *et al.*, 1983). Trichomes may play roles in the detoxification of heavy

metals. The evidence showed decreased stomata density, increased stomata size and especially the spreading and shape of trichomes on the adaxial and abaxial epidermises. In contrast with sunflower, the plants growing in tannery sludge (containing Cr, Fe, Zn and Mn) showed an increase in the frequency of stomata and trichomes (Singh and Sinha, 2004). Trichomes are specialized unicellular or multicellular structures derived from the epidermal cell layer, which may have various functions depending on the plant species and organ (Rodriguez *et al.*, 1983). Trichomes may play roles in the detoxification of heavy

Table 3. Leaf anatomical characters of *M. spectabilis* growing in Zn/Cd contaminated and non-contaminated soils.

Characteristics		Leaves of plants growing in non-contaminated soil		Leaves of plants growing in Zn/Cd contaminated soil	
		adaxial	abaxial	adaxial	abaxial
Density of stomata/mm ²	margin	6.76±1.35*	47.05±5.32 ^a	3.69±1.16**	43.58±4.34 ^a
	midrib	-	36.08±6.55 ^a	-	37.44±5.40 ^a
Stomata size (µm)	margin	43.40±3.81**	45.63±4.22 ^b	45.75±2.68*	48.39±5.11 ^a
	midrib	-	54.59±4.40 ^a	-	49.21±2.92 ^b
Macro-hairs (µm)	margin	291.04±83.64*	206.39±57.83	252.83±59.15*	-
Micro-hairs (µm)	margin	108.64±22.11*	101.11±28.10	97.65±16.42*	-
Trichome shapes	margin	UT, UGT	UT, UGT	UT	-
	midrib	UT, UGT	UT, UGT	-	-

UT = Uniseriate non-glandular trichomes; UGT = uniseriate glandular trichomes

Data is means±SD (n=30). Those with different superscript letters in the same row are significantly different (p<0.01).

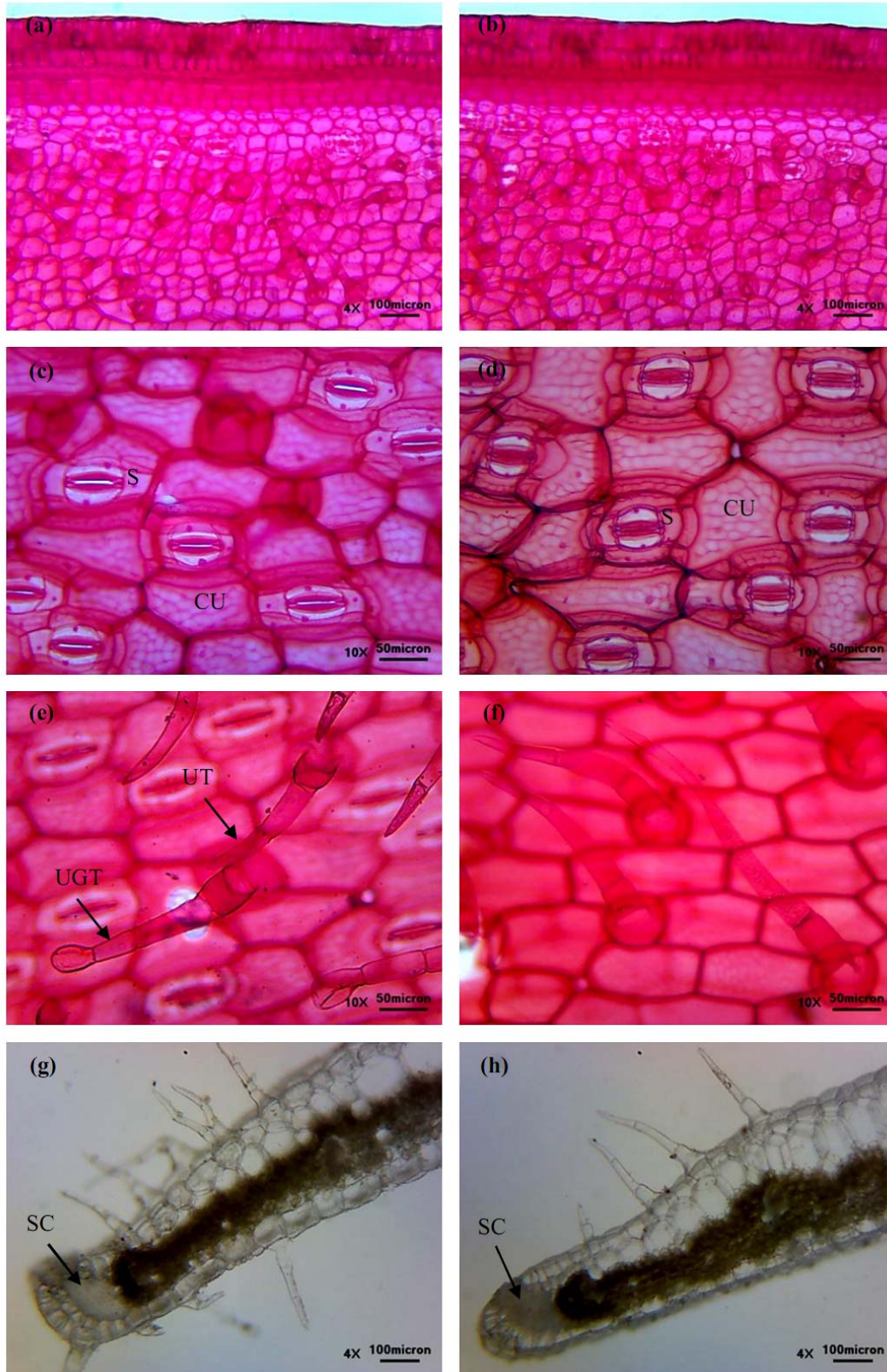


Figure 2. Leaf anatomical features of *M. spectabilis*: (a) and (b) marginal adaxial epidermis; (c) and (d) hexacytic stomata; (e) and (f) trichome shapes; (g) and (h) transverse section of marginal region. a, c, e and g were *M. spectabilis* grown in non-contaminated soil and b, d, f and h were *M. spectabilis* growing in Zn/Cd contaminated soil. Abbreviations and symbols: CU, cutin; S, stoma; SC, sclerenchyma; UT, uniseriate non-glandular trichome; UGT, uniseriate glandular trichome.

Table 4. Percentages of elements in leaves of *M. spectabilis* growing in Zn/Cd contaminated and non-contaminated soils (control), studied by SEM/EDS.

Elements	% elements in epidermis		% elements in vascular bundle		% elements in cross section	
	Treatment	Control	Treatment	Control	Treatment	Control
C	55.2±1.7	53.0±1.2	51.5±1.3	46.2±0.5	54.0±2.3	48.7±1.2
O	42.6±0.9	43.2±0.3	39.9±1.0	44.5±1.7	37.3±1.1	41.7±1.5
Mg	0.2±0.2	0.9±0.5	0.5±0.1	1.5±0.3	0.6±0.2	1.4±0.2
Si	0.50±0.3	0.8±0.2	0.5±0.1	1.1±0.1	0.3±0.1	1.2±0.3
S	0.04±0.06	N/D	0.4±0.2	0.5±0.3	0.3±0.0	0.3±0.4
Cl	0.9±0.3	1.8±0.8	4.7±0.2	4.9±1.1	4.9±0.7	5.4±0.4
Ca	0.4±0.2	0.3±0.1	1.9±0.3	1.4±0.4	2.3±0.8	1.3±0.4
Zn	0.02±0.01	N/D	0.2±0.04	N/D	0.1±0.01	N/D
Cd	0.1±0.04	N/D	0.3±0.1	N/D	0.1±0.04	N/D
Total	100	100	100	100	100	100

Mean values ($n = 3$) ± standard deviation (S.D.), N/D = not detectable

metals, and in response to various other stress conditions. The accumulation of Zn and/or Cd in trichomes of dicots have been reported in *P. divaricata* (Broadhurst *et al.*, 2013; Hu *et al.*, 2012), tobacco (Sarret *et al.*, 2006; Choi *et al.*, 2001), *A. thaliana* (Isaure *et al.*, 2006) and *A. halleri* (Sarret *et al.*, 2002; Zhao *et al.*, 2000; Küpper *et al.*, 2000; Fukuda *et al.*, 2008). However, symptoms of phytotoxicity in plants, especially distribution and accumulation of Zn and Cd in trichomes depends on the metals concentrations in treatments (Sridhar *et al.*, 2007; Nakbanpote *et al.*, 2010). In addition, Choi *et al.* (2004) reported the uniserate short and long glandular trichomes, with a multi-cellular head in tobacco that had different functional activity, as short trichomes for Cd exudation and long trichomes for NaCl sequestration. In this research, the uniserate glandular trichomes of *M. spectabilis* were missing from the abaxial epidermis [Fig. 2(h), Fig. 4(c)], and the only remaining evidence was flattening trichomes [Fig. 4(e)]. Therefore, the glandular trichomes might primarily respond to Zn/Cd detoxification of *M. spectabilis*.

Based on the leaf cross sections, SEM/EDS indicated an increase of Ca in leaves of *M. spectabilis* corresponding to Zn and Cd distribution in the epidermis and vascular bundle (Table 4). The increase of S and Ca under Cd treatment revealed by EDS was also reported in the short trichomes of tobacco (Choi *et al.*, 2004). The positive effect of Ca on Zn tolerance results from a cooperative, and not an inhibitive, mechanism between the two elements (Sarret *et al.*, 2006). The Zn and Cd accumulation in the tip cell of the glandular trichomes and the chemical forms of the exudated grains as metal-substituted calcite have been reported in tobacco (Harada and Choi, 2008; Sarret *et al.*, 2006). The percentages of Zn and Cd in the vascular bundle are much stronger than

in the cross section and epidermis areas, respectively (Table 4). As solutes (Zn and Cd) were selectively taken up at the bundle sheath plasma membrane into the leaf symplast, both solutes could move along each route with diffusion through the symplast (cell-to-cell movement) being driven by osmotic gradients created as solutes are actively transported across membranes, with transpirational flow being the dominant force influencing the movement through the apoplast (Karley *et al.*, 2000).

3.3. X-ray absorption near-edge structure (XANES) of zinc and sulphur

The XANES spectra of the tuber epidermis (TU-E), cortex and vascular cylinder (TU-I) and leaves of *M. spectabilis* growing in Zn/Cd contaminated soil were investigated to obtain information on the oxidation state and possible geometric structure of Zn and S atoms. The Zn K-edge XANES spectra of the bulk plant samples indicated the oxidation state as +2. The adsorption edge energy was close to the edge of the Zn-cysteine and ZnSO₄ (data not shown). However, the shapes of the Zn XANES spectra had one peak that was difficult to determine. The XANES of the sulfur K-edge was investigated to obtain the possible geometric structure of sulfur on the samples. The normalized XANES spectra of the S K-edge in the plant samples and the reference materials are shown in Fig. 5. In this research, the positions of the adsorption edge energy were defined by the second derivative XANES spectra [Fig. 5(b)]. The adsorption edge energy of the S K-edge XANES spectra of the tuber (TU-E and TU-I) and leaves was 2473.3 eV, and the shapes of the XANES spectra had triple peaks (2473.3 eV, 2476 eV and 2481 eV). The

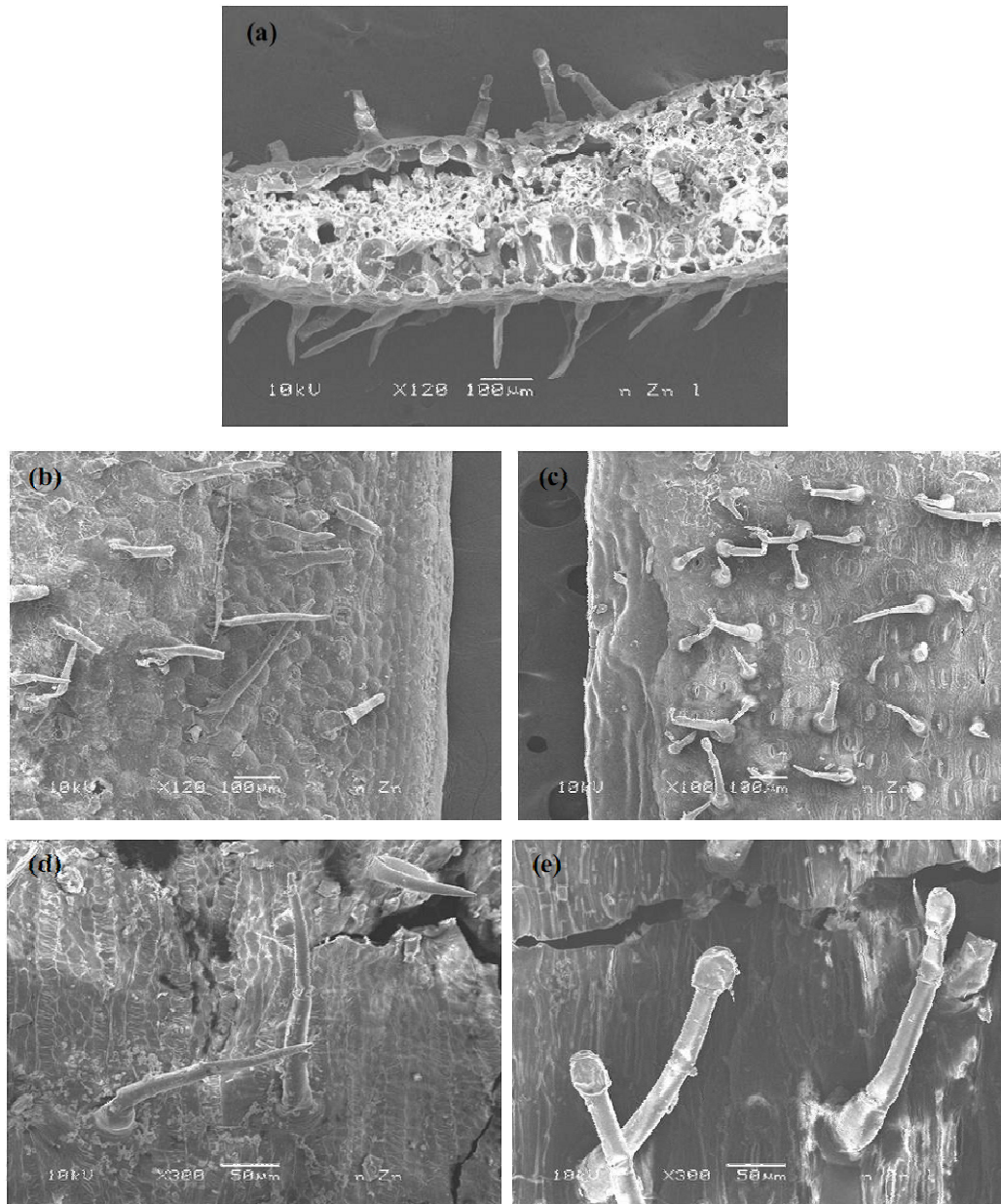


Figure 3. SEM images of trichomes on the leaves of *M. spectabilis* growing in non-contaminated soil (control); (a) transverse section of midrib region, (b) adaxial epidermis, (c) abaxial epidermis, and (d) and (e) high magnification view showing non-glandular and glandular trichomes, respectively.

triple peaks of TU-E and leaves might relate to the mixtures of $ZnSO_4$ and Zn-cysteine, in which the double peaks at 2473.3 eV and 2476 eV could indicate the Zn-cysteine (Panitlertumpai *et al.*, 2013). The double peaks of the Zn-cysteine dominated in the leaves more than TU-E. In addition, the height and shape of the S K-edge XANES spectrum of TU-I tended to associate mainly with $ZnSO_4$.

Xylem-unloading processes might be the first step in controlled distribution of metals from root to shoot. Thus, chelation with certain ligands of organic acid(s), for example, citrate and histidine, appears to be the route metals primarily take to the xylem and for metal homeostasis in the roots (Clemens *et al.*, 2002; Salt

et al., 1999). In contrast, chelation with other ligands, such as phytochelatins or metallothioneins, might be the route metals predominately take to sequestration in the leaves (Clemens *et al.*, 2002). Therefore, Zn K-edge and S K-edge XANES spectra propose that Zn^{2+} ions are accumulated and/or adsorbed on the epidermis of the tuber, and then Zn^{2+} uptake occurs in the root and there is transport to the xylem. The peak at 2481 eV correlating with $ZnSO_4$ might occur due to the Zn^{2+} binding to SO_4^{2-} in the plant cells during the freeze-drying of the samples. The strong expression of double peaks of Zn-cysteine in the leaf samples indicated the sequestration by sulphur ligand proteins. In which, one of the strategies for plants to resist the toxicity of

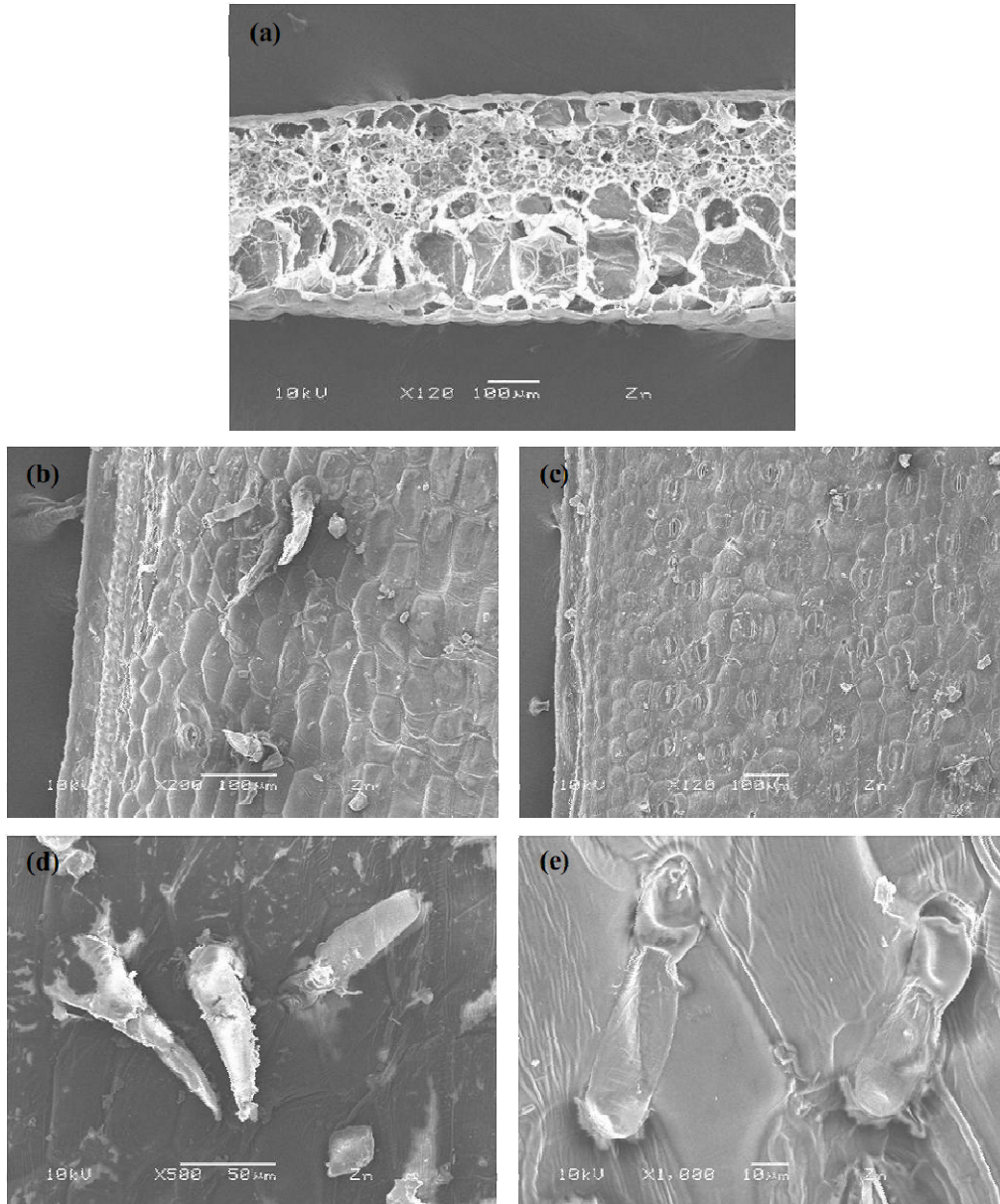


Figure 4. SEM images of trichomes on the leaves of *M. spectabilis* growing in Zn/Cd contaminated soil; (a) transverse section of midrib region, (b) adaxial epidermis, (c) abaxial epidermis, and (d) and (e) high magnification view showing the effect of Zn/Cd on trichome shapes.

Zn and Cd is complexation with strong ligands, such as thiol groups provided by cysteine, and amino-acid constituting peptides often mentioned, namely glutathione, phytochelatins and metallothioneins (Cobbett and Goldsbrough, 2002).

4. Conclusion

The Zn/Cd soil sample collected from Mae sot, Tak Province, Thailand contained extractable Zn and Cd concentrations as high as 1,290 and 8.65 mg/kg dry weight, respectively. *M. spectabilis* growing in the contaminated soil accumulated Zn and Cd in shoot (stem and leaves) at levels of 2,067.1 mg/kg dry weight and

26.7 mg/kg dry weight, respectively. From the criteria of metal accumulation, translocation factor (*TF*) and bioaccumulation factor (*BF*), *M. spectabilis* could be indicated as a Zn/Cd hyperaccumulative plant. The microscopic studies showed the effect of Zn and Cd on the morphological of the leaves of *M. spectabilis*. The included decreased stomata density, increased stomata size, and especially spreading and shape of the trichome on the adaxial and abaxial epidermises. The uniseriate glandular trichome was absent from the abaxial epidermis of the plants' leaves growing in the contaminated soil, and remained the only evidence of the flattening of the glandular trichomes. Therefore, the glandular trichomes played important roles in the detoxification of Zn and

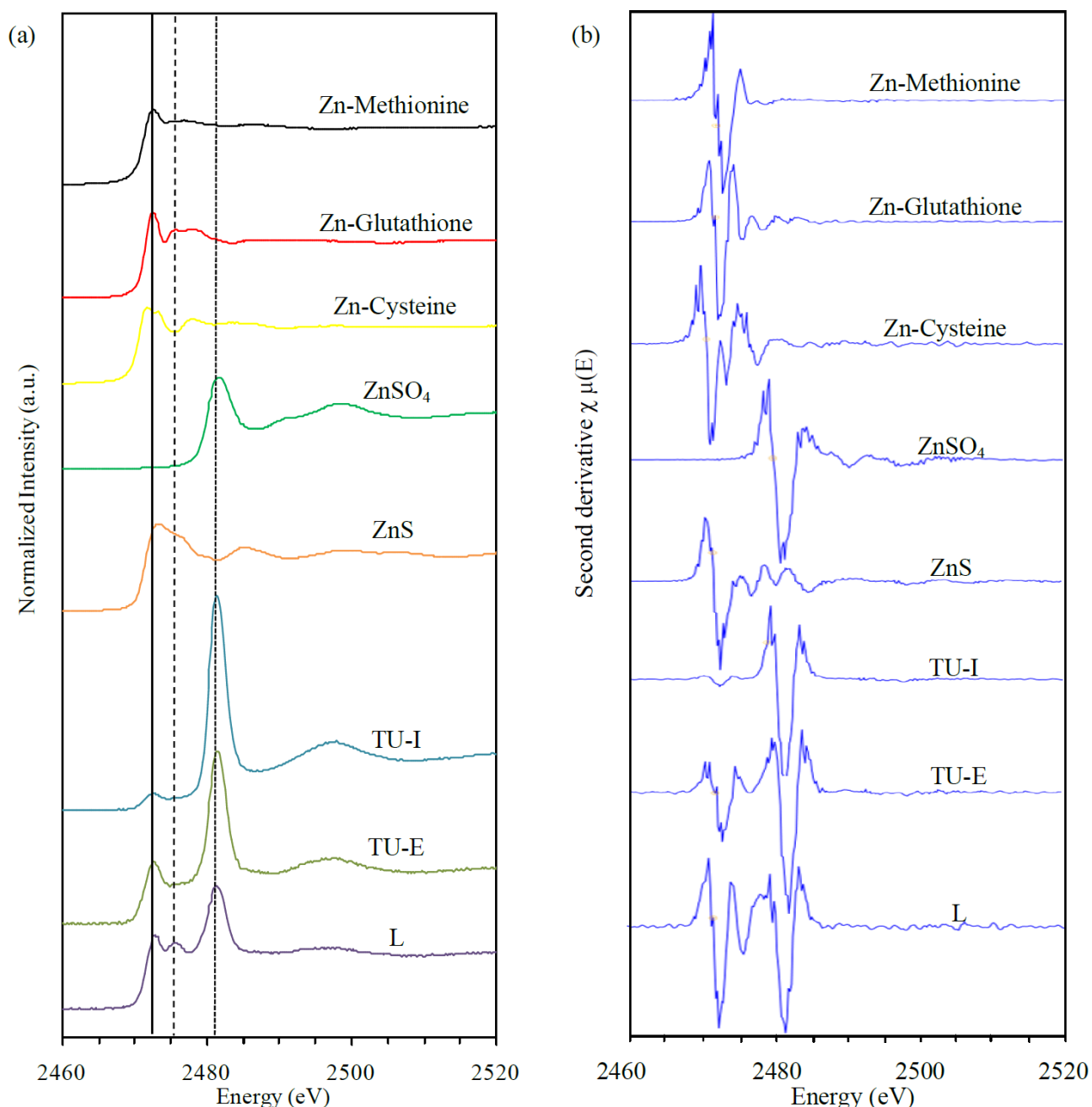


Figure 5. Normalized (a) and second derivative, (b) S K-edge XANES spectra of the tuber and leaves of *M. spectabilis* growing in Zn/Cd contaminated soil. The reference materials (ZnS, ZnSO₄, Zn-cysteine, Zn-glutathione and Zn-methionine) are shown. L = leaves, TU-E = epidermis of tuber, TU-I = cortex and vascular cylinder of tuber.

Cd in the plants. The higher percentages of Zn and Cd in the vascular bundle than that in the cross section and epidermis areas showed both solutes could diffuse from the xylem to the mesophyll and epidermis through the symplast and apoplast. The increase of Ca corresponding to the Zn and Cd distributed in the leaves implied that Cd might be involved in the metal sequestration in leaves. Zn K-edge and S K-edge XANES spectra proposed that transportation of Zn²⁺ ions from swollen roots (tubers) to the xylem and leaves. The triple peaks

of TU-E, TU-I and leaves might relate to the mixtures of ZnSO₄ and Zn-cysteine, in which the double peaks at 2473.3 eV and 2476 eV could indicate Zn-cysteine. The obvious double peaks of Zn-cysteine in the leaf samples indicated metal sequestration by sulfur proteins. Finally, SEM/EDS analysis, μ -X-ray fluorescence (XRF) imaging and μ -XANES will be performed in further studies to determine the constituents and distribution of the Zn, Cd and other elements, such as Ca, S and Si in the leaf morphology, especially trichomes.

Acknowledgements

The authors would like to thank the Synchrotron Light Research Institute (Public Organization) for research facilities at beamline 8 (XAS), and be grateful to Asst. Prof. Dr. Taweesak Thitimetharoch for plant identification, and Dr. Jolyon Dodgson for English proofreading. Rattanapolsan, L. gratefully thanks the Human Resource Development in Science Project (Science Achievement Scholarship of Thailand, SAST).

References

- American Society for Testing and Materials. Standard test methods for copper in iron ores by atomic absorption spectroscopy. Annual Book of ASTM Standard, Philadelphia, ASTM 2004; E841-04.
- Alloway BJ, Heavy Metals in Soils, 2nd ed. Blackie Academic & Professional, Glasgow, 1995.
- Baker AJM, Ewart K, Hendry GAF, Thorpe PC, Walker PL. The evolutionary basis of cadmium tolerance in higher plants. *In: Proceeding of the 4th International Conference on Environmental Contamination (Ed: Barcelo J)*. CEP Consultants Ltd, Barcelona, 1990; 23.
- Baker AJM, Whiting SN. In search of the holy grail-a further step in understanding metal hyperaccumulation. *New Phytologist* 2002; 155: 1-7.
- Barber SA. Soil nutrient bioavailability: a mechanistic approach. 2nd ed. John Wiley & Sons, New York, USA. 1995; 414.
- Bowen HJM, Environmental chemistry of the elements, Academic Press, New York, 1979.
- Branquinho C, Serrano HC, Pinto MJ, Martins-Loução MA. Revisiting the plant hyperaccumulation criteria to rare plants and earth abundant elements. *Environmental Pollution* 2007; 146: 437-43.
- Broadhurst CL, Bauchan GR, Murphy CA, Tang YT, Pooley C, Davis AP, Chaney RL. Accumulation of Zinc and Cadmium and Localization of Zinc in *Picris divaricata* Vant. *Environmental and Experimental Botany* 2013; 87: 1-9.
- Chaney RL. Zinc phytotoxicity. *In: Zinc in soils and Plants (Ed: Robson AD)*, Kluwer Academic Publishers, Dordrecht, 1993; 135-50.
- Choi YE, Harada E, Wada M, Tsuboi H, Morita Y, Kusano T, Sano H. Detoxification of cadmium in tobacco plant: formation and active excretion of crystals containing cadmium and calcium through trichomes. *Planta* 2001; 213: 45-50.
- Choi YE, Harada E, Kim GH, Yoon, Sano H. Distribution of elements on tobacco trichomes and leaves under cadmium and sodium stresses. *Journal of Plant Biology* 2004; 47: 75-82.
- Clemens S, Palmgren MG, Krämer U. A long way ahead: understanding and engineering plant metal accumulation. *Trends in Plant Science* 2002; 7: 309-15.
- Cobbett C, Goldsbrough P. Phytochelatin and metallothioneins: Roles in heavy metal detoxification and homeostasis. *Annual Plant Biology* 2002; 53: 159-82.
- Fukuda N, Hokura A, Kitajima N, Terada Y, Saito H, Abe T, Nakai I. Micro X-ray fluorescence imaging and micro X-ray absorption spectroscopy of cadmium hyperaccumulating plant, *Arabidopsis halleri* spp. gemmifera, using high-energy synchrotron radiation. *Journal of Analytical Atomic Spectrometry* 2008; 23: 1068-75.
- González RC, González-Chávez MCA. Metal accumulation in wild plants surrounding mining wastes. *Environmental Pollution* 2006; 144: 84-92.
- Harada E, Choi YE. Investigation of metal exudates from tobacco glandular trichomes under heavy metal stresses using a variable pressure scanning electron microscopy system. *Plant Biotechnology* 2008; 25: 407-11.
- Hu PJ, Gan YY, Tang YT, Zhang QF, Jiang D, Yao N, Qiu RL. Cellular tolerance, accumulation and distribution of cadmium in leaves of hyperaccumulator *Picris divaricata*. *Pedosphere* 2012; 22: 497-507.
- Isaure MP, Fayard B, Sarret G, Pairis S, Bourguignon J. Localization and chemical forms of cadmium in plant samples by combining analytical electron microscopy and x-ray spectromicroscopy. *Spectrochimica Acta Part B: Atomic Spectroscopy* 2006; 61: 1242-52.
- Johansen DA. *Plant Microtechnique*. McGraw-Hill Book Company, New York, USA 1940.
- Kabata-Pendias A, Pendias H. *Trace Element in Soils and Plant*, 2nd ed. CRC Press, Florida, 1992.
- Karley AJ, Leigh RA, Sanders D. Where do all the ions go? The cellular basis of differential ion accumulation in leaf cells. *Trends in Plant Science* 2000; 5: 465-70.
- Küpper H, Lombi E, Zhao FJ, McGrath SP. Cellular compartmentation of cadmium and zinc in relation to other metal in the hyperaccumulator *Arabidopsis halleri*. *Planta* 2000; 212: 75-84.
- Lindsay WL, Norvell WA. Development of a DTPA soil test for zinc, iron, manganese, and copper. *Soil Science Society of America Journal* 1978; 42: 421-28.
- Miller, RO. Nitric-perchloric acid wet digestion in an open vessel. *In: Handbook of reference methods for plant analysis (Ed: Kalra YP)*. CRC Press, Boca Raton, U.S.A 1998; 57-61.
- Nakbanpote W, Panitertumpai N, Sukadeetad K, Meesungneon O., Noisa-nguan W. Advances in phytoremediation research: A case study of *Gynura pseudochina* (L.) DC. *In: Advanced knowledge application in practice (Ed: Fürstner I)*. SCIYO, Croatia. 2010; 353-78.
- Panitertumpai N, Nakbanpote W, Thiravetyan P, Surarungchai W. "The exploration of zinc-hyperaccumulative plants from mining area of Tak province in Thailand", *Proceeding in the 29th Congress on Science and Technology of Thailand, 20-22 October, KhonKaen University, KhonKaen, Thailand 2003*.
- Panitertumpai N, Nakbanpote W, Sangdee A, Thumanu K, Nakai I, Hokura A. Zinc and/or cadmium accumulation in *Gynura pseudochina* (L.) DC. Studied in vitro and the effect on crude protein, *Journal of Molecular Structure* 2013; 1036: 279-91.
- Phaenark C, Pokethitiyook P, Kruatrachue M, Ngernsarsaruay C. Cd and Zn accumulation in plants from the padaeng zinc mine area. *International Journal of Phytoremediation* 2009; 11: 479-95.

- Prasad MNV. Cadmium toxicity and tolerance in vascular plants. *Environmental and Experimental Botany* 1995; 35: 525-45.
- Rascio N, Navari-Izzo F. Heavy metal hyperaccumulating plants: How and why do they do it? And what makes them so interesting? *Plant Science* 2011; 180: 169-81.
- Roane TM, Pepper IL, Miller RM. Microbial remediation of metals. *In: Bioremediation: Principles and applications (Eds: Crawford RL, Crawford DL)*. Cambridge University Press, Cambridge. 1996; 312-40.
- Rodriguez E, Healey PL, Mehta I. *Biology and chemistry of plant trichomes*. Plenum Press, New York. 1983.
- Salt DE, Prince RC, Baker AJM, Raskin I. and Pickering IJ. Zinc ligands in the metal hyperaccumulator *Thlaspi caerulescens* as determined using X-ray absorption spectroscopy. *Environmental Science and Technology* 1999; 33: 713-17.
- Sarret G, Saumitou-Laprade P, Bert V, Proux O, Hazemann JL, Traverse A, Marcus MA, Manceau A. Forms of zinc accumulated in the hyperaccumulator *Arabidopsis halleri*. *Plant physiology* 2002; 130: 1815-26.
- Sarret G, Harada E, Choi YE, Isaure MP, Geoffroy N, Fakra S, Marcus MA, Birschwilks M, Clemens S, Manceau A. Trichomes of tobacco excrete zinc as zinc-substituted calcium carbonate and other zinc-containing compounds. *Plant Physiology* 2006; 141: 1021-34.
- Shu SZY. *Murdannia Royle*, Illustrations of the botany and other branches of the natural history of the Himalayan Mountains: and of the flora of Cashmere 1: 403. 1840, nomen conservandum. *Flora of China*, 2000; 24: 25-31.
- Simmons RW, Pongsakul P, Saiyasitpanich D, Klinphoklap S. Elevated Levels of Cadmium and Zinc in Paddy Soils and Elevated Levels of Cadmium in Rice Grain Downstream of a Zinc Mineralized Area in Thailand: Implications for Public Health. *Environmental Geochemistry and Health* 2005; 27: 501.
- Simmons RW, Noble AD, Pongsakul P, Sukreeyapongse O, Chinabut N. Cadmium-hazard mapping using a general linear regression model (Irr-Cad) for rapid risk assessment. *Environmental Geochemistry and Health* 2009; 31: 71.
- Singh S, Sinha S. Scanning electron microscopic studies and growth response of the plants of *Helianthus annuus* L. grown on tannery sludge amended soil. *Environment International* 2004; 30: 389-95.
- Sridhar BBM, Han FX, Diehl SV, Monts DL, Su Y. Effects of Zn and Cd accumulation on structural and physiological characteristics of barley plants. *Brazilian Journal of Plant Physiology* 2007; 19: 15-22.
- Thitimetharoch T. Taxonomic studies of Family Commelinaceae in Thailand. Doctor of Philosophy Thesis in Biology, Graduate School, KhonKaen University. 2004.
- Zhao FJ, Lombi E, Breedon T, McGrath SP. Zinc hyperaccumulation and cellular distribution in *Arabidopsis halleri*. *Plant, Cell and Environment* 2000; 23: 507-14.

Received 23 May 2013

Accepted 10 June 2013

Correspondence to

Assistant Professor Dr. Woranan Nakbanpote
Department of Biology, Faculty of Science,
Mahasarakham University,
Khamriang, Kantarawichi District,
Maha Sarakham 44150
THAILAND
Email: woranan.n@msu.ac.th
Tel: +66 43 754321 ext. 1163